

1 **ENDORSE: a prognostic model for endocrine therapy response in advanced**
2 **estrogen-receptor positive breast cancers**

3 Aritro Nath¹, Adam L. Cohen² and Andrea H. Bild^{1*}

4

5 ¹ Department of Medical Oncology and Therapeutics, City of Hope Comprehensive
6 Cancer Institute, Monrovia, California

7 ² Neuro Oncology Program, Inova Schar Cancer Institute, Fairfax, Virginia

8

9 *Correspondence: Andrea H. Bild, Ph.D.

10 Professor, Department of Medical Oncology and Therapeutics

11 City of Hope Comprehensive Cancer Institute

12 1218 S Fifth Ave, Monrovia, CA 91016

13 (626) 218-6052

14 abild@coh.org

15

16 Conflict of interest statement: The authors declare no potential conflicts of interest.

17 **ABSTRACT**

18 Endocrine therapy remains the primary treatment for advanced and metastatic estrogen
19 receptor-positive (ER+) breast cancers. Patients who progress on endocrine therapy
20 may benefit from add-on treatment targeting the PI3K/MTOR signaling pathways or by
21 switching to chemotherapy. However, these options are only available after progression
22 on first-line treatment with endocrine therapy. In the absence of reliable prognostic tests
23 for advanced ER+ breast cancers, it is currently not possible to stratify patients into
24 pertinent treatment arms at the baseline. To address this, we have developed a low-
25 dimensional endocrine response signature (ENDORSE) model for advanced ER+
26 breast cancers. The ENDORSE model was developed using the baseline tumor
27 transcriptomes and long-term survival outcomes of >800 invasive ER+ breast cancers
28 and predicts the risk of death on endocrine therapy. ENDORSE was validated in
29 multiple clinical trial datasets for endocrine therapy response in metastatic ER+ breast
30 cancers and demonstrated superior predictive performance over clinical factors and
31 published gene signatures. Our results show that ENDORSE is a reproducible and
32 accurate prognostic model for endocrine therapy response in advanced and metastatic
33 ER+ breast cancers.

34

35 INTRODUCTION

36 Breast cancer is the most common form of cancer globally, with more than two million
37 cases diagnosed in 2020¹. Pathogenesis and classification of breast cancer is based on
38 the presence or absence of estrogen receptor alpha (ER), progesterone receptor (PR)
39 and human growth factor-neu receptor (HER2). These subtypes guide the selection of
40 systemic therapy for breast cancer patients. More than 70% of breast cancers express
41 ER and are negative for HER2 (ER+/HER2-)^{2,3}. The primary systemic therapy for
42 ER+/HER2- breast cancer is endocrine therapy, which counters the growth of tumors by
43 targeting their dependency on estrogen signaling⁴. This includes selective estrogen
44 receptor modulators (SERMs) such as tamoxifen and selective estrogen receptor
45 degraders (SERDs) such as fulvestrant that directly prevent ER activation, or aromatase
46 inhibitors like exemestane and anastrozole that reduce circulating levels of estrogen in
47 the body^{5,6}. Endocrine therapy substantially reduces the risk of recurrence within 5-
48 years, although chemotherapy may be recommended for some patients with high risk of
49 recurrence. While clinicopathological features are not reliable predictors of recurrence
50 risk, gene expression-based genomic tests that predict the risk of recurrence can aid in
51 deciding whether the benefit of adding chemotherapy outweighs its side effects in
52 certain patients^{7,8}. These biomarkers have been validated and recommended for
53 clinical use only in early stage, node-negative cancers based on guidelines from the
54 American Society of Clinical Oncology and European Group on Tumor Markers^{9,10}.

55

56 Locally advanced and metastatic ER+ breast cancers often develop resistance to
57 endocrine therapy with significantly higher rates of recurrence and death compared to

58 early-stage disease. Despite these challenges, single-agent endocrine therapy or in
59 combination with CDK4/6 inhibitors remains the primary systemic therapy
60 recommended for locally advanced and metastatic breast cancers¹¹. Patients may
61 benefit from the addition of targeted inhibitor against the mTOR or PI3K pathways^{12,13} or
62 switching to chemotherapy¹¹. However, these treatment options are recommended for
63 consideration only upon progression on endocrine therapy, according to the American
64 Society for Clinical Oncology¹⁴, National Comprehensive Cancer Network^{15,16} and
65 European Society for Medical Oncology¹⁷ clinical practice guidelines. Therefore, the
66 ability to predict the potential benefit from first-line endocrine therapy may be crucial for
67 locally advanced and metastatic ER+ breast cancers that may benefit from continued
68 endocrine therapy, a combination treatment or chemotherapy as the primary treatment
69 strategy.

70
71 Unlike early stage, node-negative disease, genomic tests for endocrine therapy
72 response are not available for advanced and metastatic ER+ breast cancers. To
73 address this limitation, a few attempts have been made so far to develop a genomic
74 signature of endocrine response in ER+ metastatic breast cancers (ER+ MBC)^{18,19}. The
75 TransCONFIRM trial evaluated the transcriptomes of 112 ER+/HER2- MBCs and
76 identified a set of 37 genes that were associated with progression-free survival (PFS) of
77 patients receiving fulvestrant¹⁹. Another study analyzed the transcriptomes of 140
78 ER+/HER2- MBC on endocrine therapy to develop SET ER/PR, an 18-gene predictive
79 score for endocrine therapy sensitivity¹⁸. While both the TransCONFIRM and SET
80 ER/PR biomarkers predicted endocrine response in their respective training datasets,

81 neither study performed systematic validation of their predictive signatures to
82 demonstrate the reproducibility and accuracy in independent clinical datasets. This
83 issue highlights a critical flaw in biomarker development pipelines and is one important
84 reason why genomic biomarkers are infrequently translated into clinical practice²⁰.
85 Another pervasive issue hindering clinical translation arises from the reliance on a large
86 number of predictive features in complex models that are difficult to interpret and often
87 perform poorly in independent validation due to overfitting^{21,22}.

88
89 Here we developed ENDORSE: a low-dimensional expression-based prognostic model
90 for endocrine therapy and systemically tested its performance and predictive ability in
91 multiple-independent clinical trials against other diagnostic models and genomic
92 signatures. ENDORSE was developed and trained using the tumor transcriptomes and
93 overall survival (OS) of more than 800 ER+ breast cancers on endocrine therapy^{23,24}.
94 We validated the ENDORSE model in multiple independent clinical trial datasets,
95 including the TransCONFIRM and SET ER/PR trials for endocrine therapy in metastatic
96 ER+ breast cancer. Our results show that ENDORSE reproducibly predicts endocrine
97 response in independent validation clinical studies, and consistently outperforms all
98 other models of endocrine therapy response in metastatic ER+ breast cancers, clinical
99 factors, and proliferation signatures.

100 **RESULTS**

101 **Developing a low-dimensional prognostic model for endocrine therapy**

102 We developed a two-component prognostic model for endocrine therapy response
103 using the tumor transcriptomes and long-term survival outcomes of 833 ER+/HER2-

104 tumors that received endocrine therapy^{23,24} (Table 1, Figure 1a). About 2 in 5 tumors in
105 this training cohort were node-positive, while more than a third of the tumors were
106 poorly differentiated, grade 3 tumors (Table 1). The two components included an
107 empirical gene signature modeled on OS (median = 10 years) and a curated gene
108 signature defining response to estrogen²⁵. Figure 1a outlines the inclusion criteria for
109 the training dataset, method for developing the empirical gene signature and the final
110 Cox proportional hazards model based on the gene set enrichments scores (GES) of
111 the two signatures. The empirical signature was developed by first performing a feature
112 selection on the training dataset using a repeated cross-validation analysis of a lasso-
113 regularized proportional hazards model. Each iteration yielded a core set of predictive
114 features that were expanded to a correlation network. The final gene signature was
115 derived from the consensus correlation network, defined as genes appearing in at least
116 50% of the cross-validation iterations (Supplementary Figure 1, Supplementary Table
117 1). In a bivariate Cox proportional hazards model of the training data, the empirical
118 signature was associated with a reduction in survival probability, while the estrogen
119 response signature was associated with improved survival (Figure 1b). The coefficients
120 for the endocrine response, or ENDORSE, model was calculated using the training
121 cohort, resulting in $ENDORSE = 1.54 \times (\text{empirical signature GES}) - (2.72 \times \text{estrogen}$
122 $\text{response GES})$. The ENDORSE model could also be used to stratify the tumors based
123 on predicted risk, for example by setting a threshold of ≥ 2 -fold relative risk of death as
124 “high-risk” and ≤ 1 risk as “low-risk”, resulting in significant differences in the Kaplan-
125 Meier survival curves across the strata ($P = 3 \times 10^{-14}$) (Figure 1c).

126

127

Table 1: Training data patient characteristics

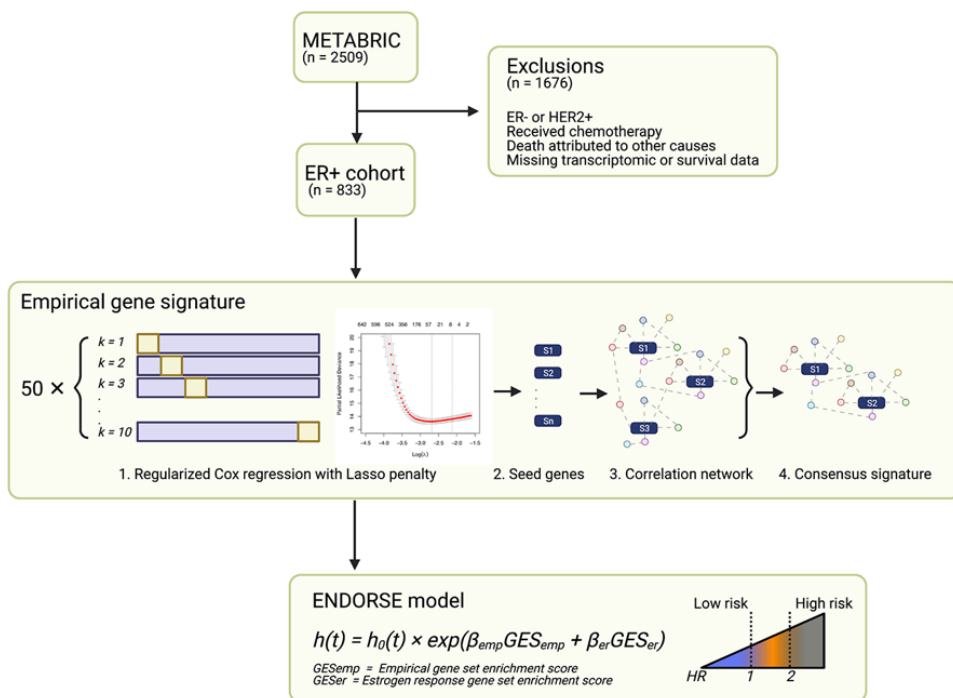
Variable	Mean	95% C.I.	N available
<i>Time to event (in months)</i>	135	130 - 140	833
<i>Events (death due to disease)</i>	0.409	0.376 - 0.443	833
<i>Age at diagnosis</i>	61.5	60.7 - 62.3	833
<i>Mutation count</i>	5.55	5.31 - 5.79	809
<i>Tumor size</i>	24.3	23.4 - 25.1	828
<i>Tumor stage</i>			
Stage 0-1 (n=270)	1.64	1.59 - 1.69	634
Stage 2 (n=324)			
Stage >3 (n=40)			
<i>Tumor Grade</i>			
Grade 1 (n=103)	2.29	2.18 - 2.27	808
Grade 2 (n=417)			
Grade 3 (n=288)			
<i>Number of positive lymph nodes detected</i>			
0 (n=491)	1.56	1.32 - 1.79	833
1-3 (n=228)			
4-9 (n=85)			
>10 (n=29)			

128

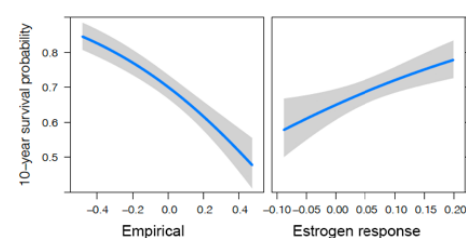
129

130

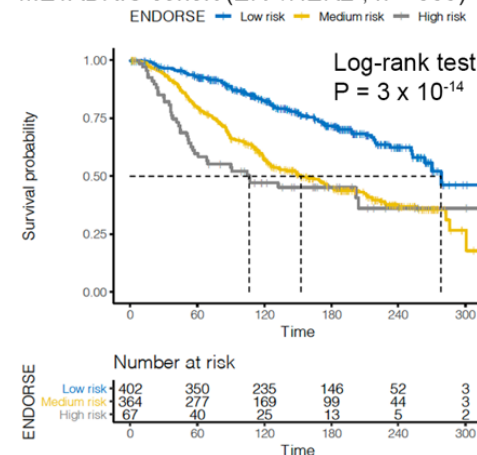
A Empirical signature development and ENDORSE model



B Predicted survival probabilities



C METABRIC cohort (ER+/HER2-, n = 833)



132 **Figure 1: ENDORSE model development in METABRIC.** A. Inclusion criteria and
 133 overall schematic of ENDORSE model development. Samples for training were selected
 134 based on ER+ status and excluded from the analysis if they were either HER2+,
 135 received chemotherapy in addition to hormone therapy, died due to other causes
 136 besides breast cancer, or were missing transcriptomic or survival data. The empirical
 137 signature was developed using a repeated cross-validation analysis framework. Each
 138 iteration of the lasso-regularized proportional hazards model generated a feature set
 139 (seed genes) predictive of OS. The seed genes were expanded to a network of
 140 intercorrelated genes, and the final empirical signature was defined by identifying a
 141 consensus set across all iterations. The two-feature ENDORSE model was then
 142 constructed using the gene set enrichment scores of the empirical signature and
 143 estrogen response signature. B. Predicted 10-year survival probabilities of the 833

144 ER+/HER2- METABRIC breast cancers based on a Cox proportional hazards model of
145 gene signature enrichment scores of the empirical and estrogen response signatures as
146 predictor variables. C. Kaplan-Meier curves and risk tables of METABRIC ER+/HER2-
147 tumors stratified by ENDORSE. The tumors were stratified according to an ENDORSE
148 risk score (hazard ratio) threshold of ≥ 2 to define high-risk, ≤ 1 as low risk and all other
149 intermediate values as medium risk.
150

151 **Internal performance evaluation, comparison with clinical covariates and**
152 **published breast cancer signatures**

153 We performed bootstrap resampling analyses to validate the Cox model in the training
154 dataset (Figure 2a) and performed likelihood ratio tests (Figure 2b) to compare with
155 other univariate prognostic models including clinical factors, proliferation index and
156 published prognostic signatures for ER+ breast cancers. First, we compared the
157 ENDORSE model to the univariate models based on the individual components of
158 ENDORSE, i.e., the empirical signature and estrogen response signature. The
159 ENDORSE model (Somers' D or $D_{xy} = 0.301$) was a better fit than the empirical
160 signature ($D_{xy} = 0.296$, $P = 1.09 \times 10^{-3}$) and the estrogen response signature ($D_{xy} =$
161 0.141 , $P = 3.93 \times 10^{-14}$) univariate models.

162
163 We then compared ENDORSE with clinical factors, such as tumor grade and mutation
164 burden. The ENDORSE model performed better than both tumor grade ($D_{xy} = 0.141$, P
165 $= 2.08 \times 10^{-3}$) and mutation count ($D_{xy} = 0.059$, $P = 9.76 \times 10^{-6}$). We also compared the
166 model with a 'meta-PCNA' proliferation index that was reported to capture the
167 prognostic ability of most published signatures of breast cancer^{26,27}. Again, the
168 ENDORSE model performed significantly better than the proliferation index ($D_{xy} =$
169 0.235 , $P = 4.42 \times 10^{-5}$), indicating its utility over measures of proliferation as a
170 prognostic tool.

171
172 Next, we evaluated published prognostic signatures for breast cancers and compared
173 their performance with ENDORSE. These signatures included PAM50, a 50-gene

174 signature that was previously reported to be a better prognostic tool for ER+ breast
175 cancers on endocrine therapy than clinical factors, such as histopathological
176 classification and tumor grade²⁸. A genomic classifier, IntClust, that developed by the
177 METABRIC consortium authors and trained on the same training dataset was also
178 included in this comparison²⁹. The PAM50 model ($D_{xy} = 0.220$) performed better than
179 IntClust ($D_{xy} = 0.153$), however the ENDORSE model outperformed both PAM50 ($P =$
180 0.033) and IntClust ($P = 0.02$) models.

181
182 Two previous clinical trials evaluating endocrine therapy response in metastatic ER+
183 breast cancers developed prognostic signatures using tumor transcriptomes. The first
184 signature developed in the TransCONFIRM trial included 37 genes that were associated
185 with PFS of advanced ER+ breast cancers on fulvestrant¹⁹. We replicated the approach
186 described in the study by performing hierarchical clustering of the samples based on the
187 expression levels of the 37 genes and cutting the tree to obtain two clusters. We
188 referred to resultant clusters as the 'TransCONFIRM' score. The TransCONFIRM score
189 applied to the METABRIC dataset performed poorly ($D_{xy} = -.002$), suggesting that the
190 signature performed no better than a random set of genes and was unsurprisingly
191 outperformed by ENDORSE ($P = 9.73 \times 10^{-6}$).

192
193 The second signature (SET ER/PR) was developed using tumor transcriptomes of
194 metastatic ER+ breast cancers on endocrine therapy¹⁸. This signature included 18
195 predictive genes that were correlated with *ESR1* or *PGR* expression and normalized
196 using 10 reference transcripts. We implemented the methods described in original study

197 and referred to the resultant score as ‘SET’. The SET score ($D_{xy} = 0.152$) performed
198 better than TransCONFIRM; however, it was also easily outperformed by ENDORSE (P
199 $= 3.53 \times 10^{-5}$).

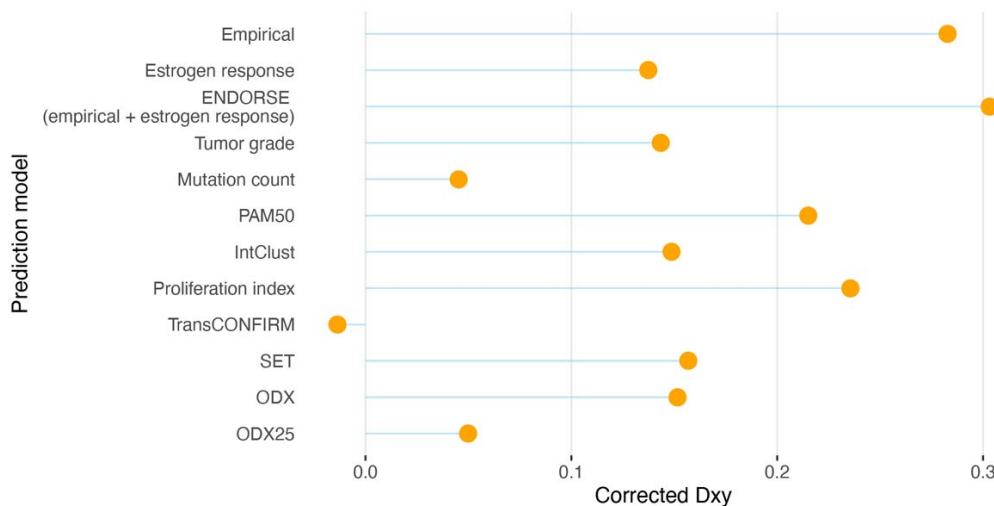
200

201 Finally, we calculated a surrogate based on the published formula for the 21-gene
202 prognostic signature approved for early-stage, node-negative ER+ breast cancers³⁰.
203 We referred to this score as ODX. We also compared a classifier that stratified samples
204 based on 25th percentile of ODX score as a proxy for the latest risk stratification
205 threshold for this signature⁸, and referred to this score as ODX25. We found that the
206 ODX model ($D_{xy} = 0.159$) was comparable to other published signatures like the SET
207 score but the stratified ODX25 score performed poorly ($D_{xy} = 0.056$). Again, the
208 ENDORSE model performed significantly better than both ODX ($P = 6.15 \times 10^{-5}$) and
209 ODX25 ($P = 1.32 \times 10^{-5}$) models. These results show that ENDORSE is significantly
210 better prognostic model than available gene signatures, clinical factors and proliferation
211 index for endocrine therapy in the METABRIC dataset.

212

METABRIC cohort (ER+/HER2-, n = 833)

A Prediction model validation (bootstrap resampling, B=150)



B Model comparisons

<i>Model 1</i>	<i>Model 2</i>	Variance test <i>H1: Model 1 and Model 2 are distinguishable</i>	Likelihood ratio test (nested) <i>H1A: Full model fits better than reduced model</i>	Partial likelihood ratio test (non-nested) <i>H1A: Model 1 fits better than Model 2</i>
<i>ENDORSE</i>	Empirical	1.47×10^{-3}	1.09×10^{-3}	
	Estrogen response	3.83×10^{-6}	3.93×10^{-14}	
<i>METABRIC tumor characteristics and signatures</i>				
	Tumor grade	$< 2 \times 10^{-16}$		2.08×10^{-3}
	Mutation count	$< 2 \times 10^{-16}$		9.76×10^{-6}
	PAM50	2.22×10^{-8}		0.033
	IntClust	$< 2 \times 10^{-16}$		0.02
	Proliferation index	3.73×10^{-5}		4.42×10^{-5}
<i>External signatures</i>				
	TransCONFIRM	1.67×10^{-7}		9.73×10^{-6}
	SET	$< 2 \times 10^{-16}$		3.53×10^{-5}
	ODX	2.18×10^{-7}		6.15×10^{-5}
	ODX25	1.49×10^{-6}		1.32×10^{-5}

213
 214 **Figure 2: Model evaluation and comparison with other predictors** a. Lollipop plots
 215 displaying corrected Somer's D_{xy} indices of ENDORSE and various other univariate Cox
 216 proportional hazards models. The indices were calculated using 150-fold bootstrap
 217 resampling of the training dataset. b. Table comparing the ENDORSE model with
 218 various other univariate Cox models using partial likelihood ratio tests. The comparison

219 between the nested ENDORSE model and its two components were performed using a
220 likelihood ratio test, while other non-nested univariate models were compared using a
221 partial likelihood ratio test.

222

223 **Validation and performance evaluation in independent clinical trial datasets**

224 To test the reproducibility and validate the performance of ENDORSE, we applied the
225 model to the baseline transcriptomes of ER+ tumors from three independent clinical
226 trials and compared the ENDORSE-predicted risk or strata with the outcomes reported
227 in each trial. These independent trials also included the TransCONFIRM and SET
228 ER/PR studies discussed earlier. So, we also compared the performance of
229 TransCONFIRM and SET scores in their respective training datasets and also across
230 other independent datasets.

231

232 The TransCONFIRM trial evaluated fulvestrant response in 112 advanced metastatic
233 ER+ breast cancers previously treated with an antiestrogen¹⁹. While the original study
234 developed and evaluated the performance of their 37-gene signature based on PFS,
235 this survival data was not made available with the publication (the authors did not
236 respond to our requests for this data). However, the study reported the post-therapy
237 resistant or sensitive states of the tumors based on histopathological staining (Ki67
238 staining). Therefore, we compared the percentage of cells positive for Ki67 staining
239 reported by in study with risk predictions from ENDORSE and other signatures (Figure
240 3). The percentage of cells positive of Ki67 were significantly correlated with the
241 ENDORSE estimated risk ($P = 2.5 \times 10^{-5}$) (Figure 3a), while stratification of the patients

242 based on the risk thresholds also showed significant difference in Ki67 staining
243 percentage between the strata ($P = 1.2 \times 10^{-3}$) (Figure 3b). However, the SET score
244 was not correlated with Ki67 staining ($P = 0.3$) (Figure 3c). The TransCONFIRM score
245 that was developed on this dataset was significant ($P = 0.05$) but performed worse than
246 the ENDORSE score trained on an independent dataset.

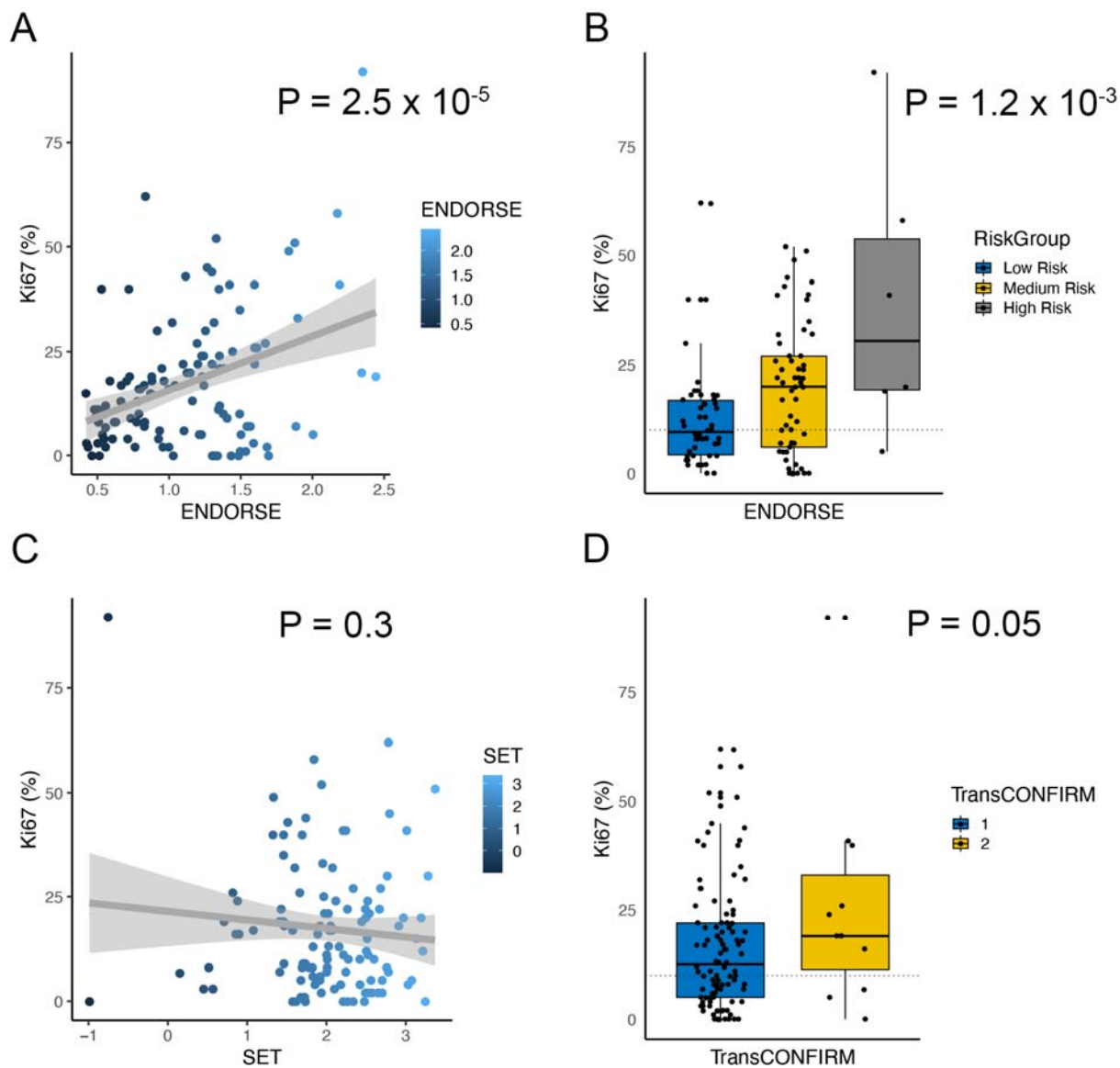
247
248 Next, we evaluated the performance of the signatures in the SET ER/PR cohort. This
249 clinical trial reported the PFS and OS of 140 stage IV ER+ metastatic breast cancers on
250 endocrine therapy. We compared the survival curves of the patients by stratifying them
251 based on the ENDORSE predicted risk, median SET scores, as described in the original
252 study, and the TransCONFIRM score. The stratification based on ENDORSE (Figure
253 4a) and SET (Figure 4b) scores both resulted in significant differences in the survival
254 curves (ENDORSE $P = 2 \times 10^{-4}$, SET $P = 3 \times 10^{-3}$). However, the TransCONFIRM score
255 (Figure 4c) was not significant ($P = 0.9$). Similarly, we observed that ENDORSE (Figure
256 4d) and SET (Figure 4e) scores both resulted in significant differences in the PFS
257 curves (ENDORSE $P = 1 \times 10^{-6}$, SET $P = 5 \times 10^{-3}$), while TransCONFIRM was not
258 significant ($P = 0.2$). Additionally, we compared the model fits using partial likelihood
259 ratio tests. The SET model that was trained using the same dataset was not a better fit
260 than the ENDORSE model (OS $P = 0.667$, PFS $P = 0.258$). The ENDORSE model was a
261 better fit than the TransCONFIRM model in each case (OS $P = 0.046$, PFS $P = 0.038$).
262 In addition to the two metastatic ER+ breast cancer trials, we also evaluated the
263 performance of the signatures examined data from the ACOSOG Z1031B clinical trial
264 which evaluated neoadjuvant aromatase inhibitor (AI) treatment in Stage II or III ER+

265 breast cancers³¹. This study reported percentage of Ki67 staining both at the study
266 baseline and at the end of treatment (2-4 weeks). We compared the percentage of Ki67
267 positive cells across cancers stratified by the ENDORSE score and found significant
268 difference across the classes at both the baseline ($P = 4.9 \times 10^{-9}$) and at the end of
269 treatment ($P = 3 \times 10^{-18}$) (Figure 5a). Similarly, the continuous ENDORSE scores were
270 significantly correlated with both the baseline ($P = 3.3 \times 10^{-15}$) and end of treatment ($P =$
271 1.1×10^{-17}) Ki67 percentage (Figure 5b). The ENDORSE scores were also significantly
272 higher in the tumors that were classified as resistant based on clinical response ($P = 4.6$
273 $\times 10^{-6}$) (Figure 5c). In this cohort, the SET score was also significantly correlated with
274 Ki67 percentage at the baseline ($P = 2.8 \times 10^{-5}$) and end of treatment ($P = 2.2 \times 10^{-4}$)
275 (Figure 5d), with significant difference in the SET scores between the resistant and
276 sensitive tumors ($P = 0.05$) (Figure 5e). The transCONFIRM scores were not significant
277 at the baseline ($P = 0.5$) and end of treatment (Figure 5f) or between resistant and
278 sensitive tumors ($P = 0.7$) (Figure 5g).

279
280 In addition to the endocrine therapy trials in ER+ breast cancer, we also applied the
281 ENDORSE risk estimates to stratify 429 ER-negative METABRIC breast cancers as
282 negative controls. Kaplan-Meier analyses show no significant difference between the
283 strata ($P = 0.26$, Supplementary Figure 2). This suggests that the ENDORSE model is
284 specific to the ER+ cohort and not a general prognostic model.

285

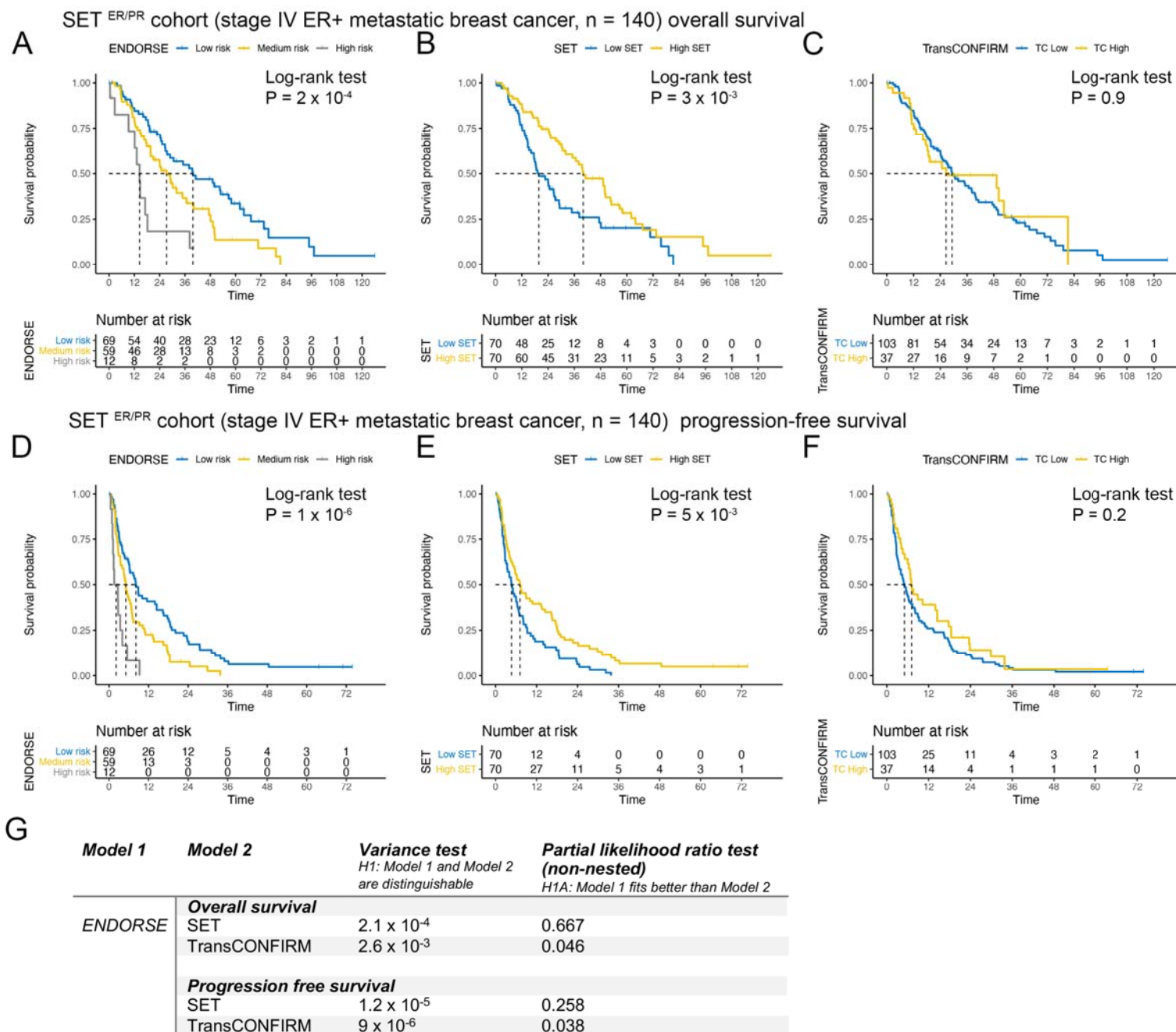
TransCONFIRM cohort (ER+ metastatic breast cancer, n = 112)



286

287 **Figure 3: Model validation in TransCONFIRM cohort.** A. Scatter plot comparing
288 ENDORSE scores (X-axis) with trial-reported percentage of cells stained positive for
289 Ki67 (Y-axis). Linear fit is shown as a grey line with shaded region showing 95%
290 confidence intervals (C.I.). P-value indicates significance of the linear fit. B. Boxplot
291 comparing Ki67 % across ENDORSE-guided patient strata. P-value indicates
292 significance of the ANOVA model and the horizontal dotted line at 10% indicates

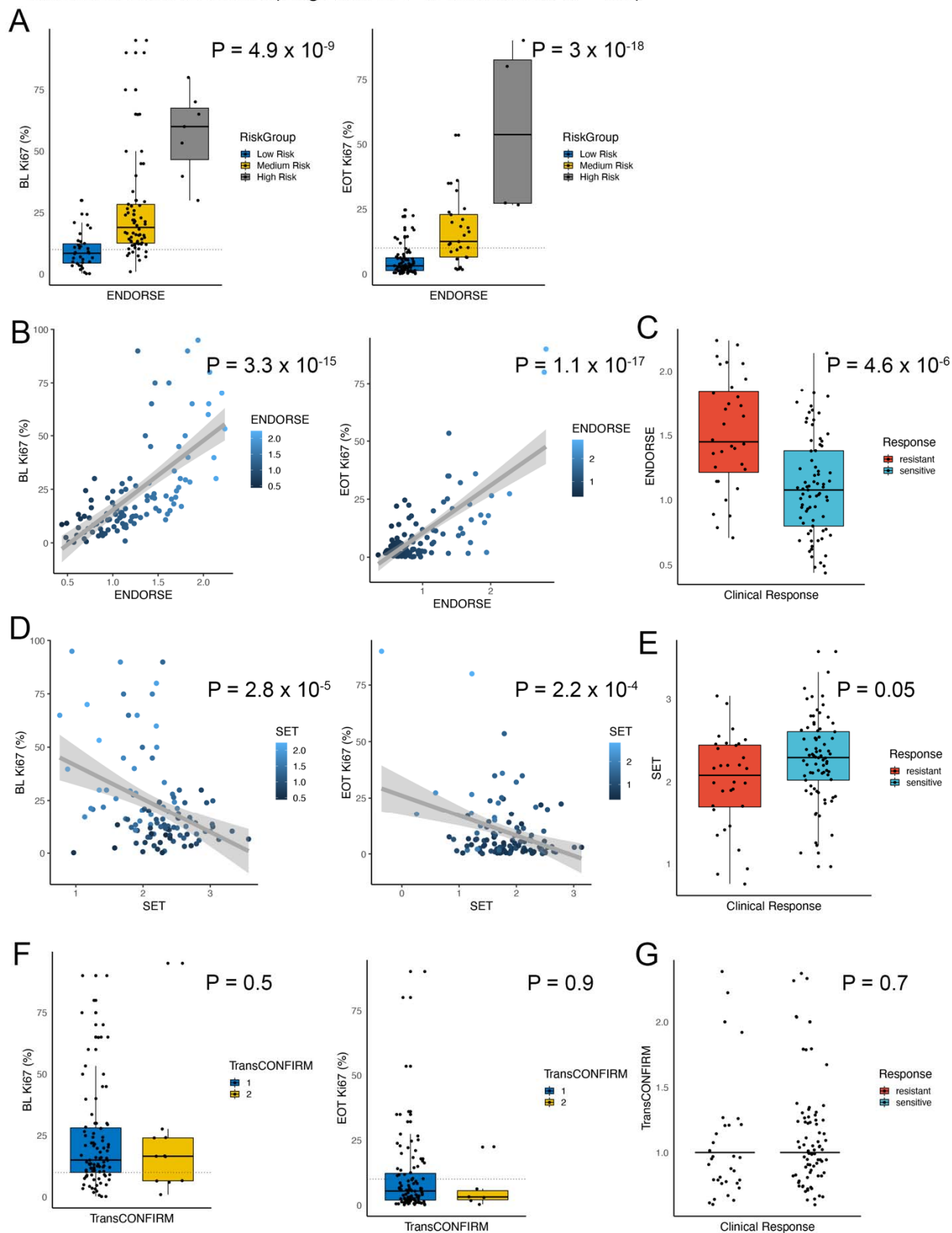
293 threshold of resistance. C. Scatter plot comparing SET scores (X-axis) Ki67 % (Y-axis).
294 Linear fit is shown as a grey line with shaded region showing 95% confidence intervals
295 (C.I.). P-value indicates significance of the linear fit. B. Boxplot comparing Ki67 %
296 across TransCONFIRM predicted patient strata. P-value indicates significance of the
297 ANOVA model and the horizontal dotted line at 10% indicates threshold of resistance.
298



300 **Figure 4: Model validation in SET ER/PR cohort.** A-C. OS Kaplan-Meier curves and
 301 risk tables of SET ER/PR patients. The patients were stratified according to A.
 302 ENDORSE B. SET and C. TransCONFIRM predicted scores. P-values indicate
 303 significance of difference in survival curves based on log-rank tests. D-F PFS Kaplan-
 304 Meier curves and risk tables of SET ER/PR patients. The patients were stratified

305 according to A. ENDORSE B. SET and C. TransCONFIRM scores. P-values indicate
306 significance of difference in survival curves based on log-rank tests. G. Table comparing
307 the ENDORSE overall and PFS models with SET and TransCONFIRM models using
308 partial likelihood ratio tests for non-nested Cox models.

ACOSOG Z1031B cohort (stage II/III ER+ breast cancer, n = 109)



310 **Figure 5: Model validation in ACOSOG Z1031B cohort.** A. Boxplots comparing Ki67
311 % at the baseline (left panel) and end of treatment (right panel) across ENDORSE-
312 predicted patient strata. P-value indicates significance of the ANOVA model and the
313 horizontal dotted line at 10% indicates threshold of resistance. B. Scatter plot comparing
314 ENDORSE scores (X-axis) and Ki67 % (Y-axis) at the baseline (left panel) and end of
315 treatment (right panel). Linear fit is shown as a grey line with shaded region showing
316 95% confidence intervals (C.I.). P-value indicates significance of the linear fit. C.
317 Boxplots comparing ENDORSE scores between patients classified as resistant or
318 sensitive clinical response. P-value indicates significance of the ANOVA model. D.
319 Scatter plot comparing SET scores (X-axis) and Ki67 % (Y-axis) at the baseline (left
320 panel) and end of treatment (right panel). Linear fit is shown as a grey line with shaded
321 region showing 95% confidence intervals (C.I.). P-value indicates significance of the
322 linear fit. E. Boxplots comparing SET scores between patients classified as resistant or
323 sensitive clinical response. P-value indicates significance of ANOVA model. F. Boxplots
324 comparing Ki67 % at the baseline (left panel) and end of treatment (right panel) across
325 TransCONFIRM-predicted patient strata. P-value indicates significance of the ANOVA
326 model and the horizontal dotted line at 10% indicates threshold of resistance. G.
327 Boxplots comparing TransCONFIRM predictions between patients classified as
328 resistant or sensitive clinical response. P-value indicates significance of ANOVA model
329
330
331

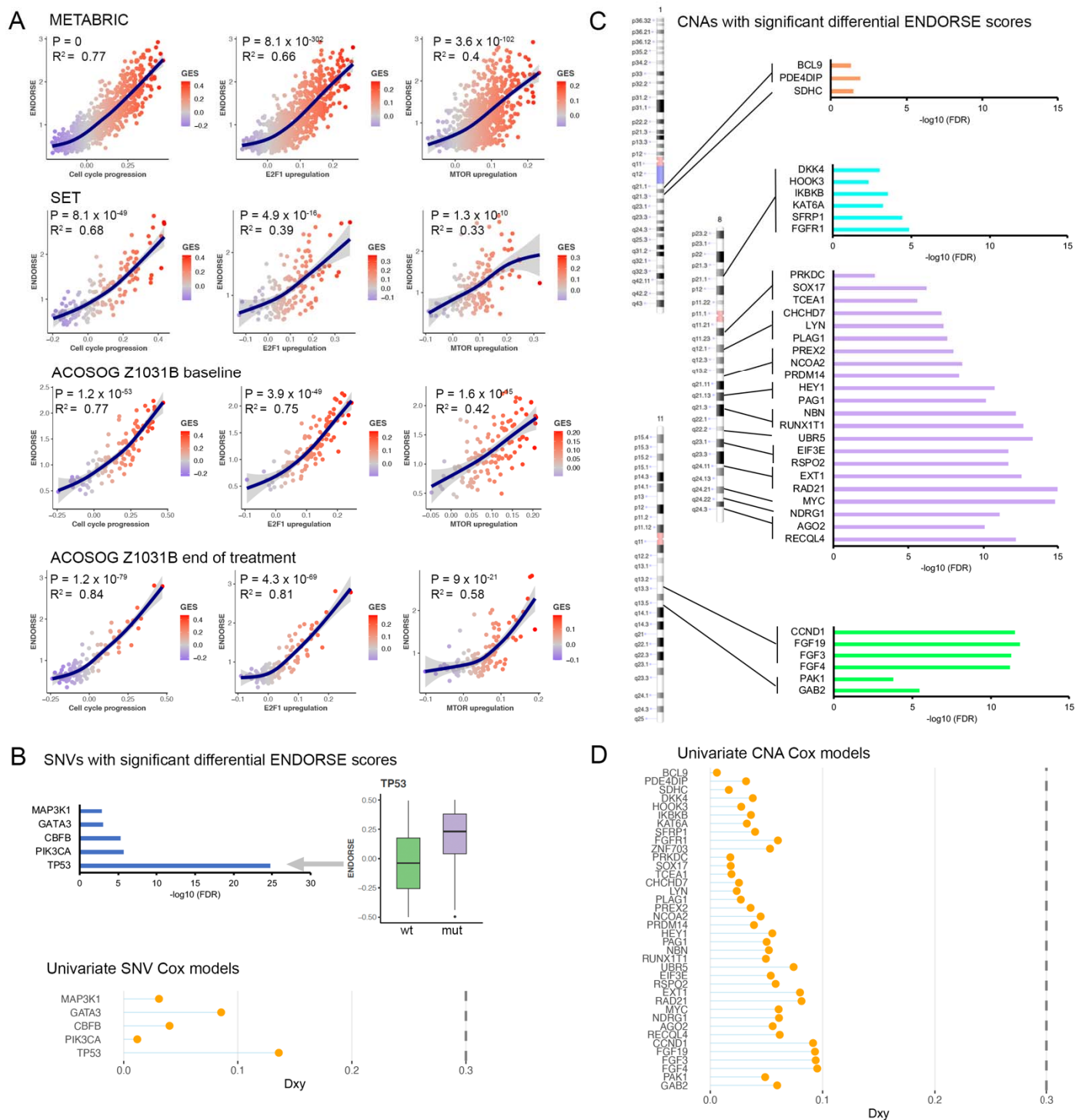
332 **Common pathway phenotypes and somatic alterations enriched in high-risk**
333 **tumors**

334 We analyzed the pathway phenotypes enriched in each dataset to identify potential
335 mechanisms that defined the high-risk tumors. First, we calculated the GES for 50
336 hallmark, 4690 curated and 189 oncogenic signatures from the METABRIC
337 transcriptomes and fitted a generalized additive model for ENDORSE scores with each
338 signature as the predictor (Supplementary Tables 2-4). We found multiple hallmark
339 signatures and oncogenic pathways to be significantly associated with the ENDORSE
340 scores (Supplementary Tables 2-4). Key enriched hallmark signatures included MTOR
341 signaling ($P = 1.03 \times 10^{-72}$) and MYC targets (v2, $P = 2.66 \times 10^{-83}$), while key oncogenic
342 signatures included gain in E2F1 target expression ($P = 8.06 \times 10^{-302}$) and loss of RB1
343 activity via p107 and p130 ($P = 9.51 \times 10^{-137}$, 1.31×10^{-67}) (Supplementary Tables 2, 4).
344 Next, we calculated the GES for the hallmark and oncogenic signatures in the three
345 validation datasets (Supplementary Tables 5-10). We observed that pathways
346 associated with cell-cycle progression and proliferation, along with signatures for the
347 loss of RB-1 activity and activation of the PI3K/AKT/MTOR signaling pathways were
348 generally enriched across the METABRIC and all the three validation datasets (Figure
349 6a). Similar to the training dataset, we also found gain in cell cycle progression along
350 with MTOR signaling and E2F1 target expression to be associated with high ENDORSE
351 scores across all datasets (Figure 6a, Supplementary Tables 5-10). The commonality of
352 the signatures enriched across different datasets suggested similar underlying
353 phenotypes were acquired by the high-risk tumors.

354 We also analyzed the association between gene-level somatic mutations, including non-
355 synonymous single-nucleotide variants (SNV) and copy number alterations, with the
356 ENDORSE scores of the METABRIC ER+ tumors. We found a statistically significant
357 association (FDR < 0.05) between the ENDORSE scores and SNVs of only five genes
358 (Figure 6b, Supplementary Table 11). While *PIK3CA* mutations were found in ~50% of
359 all tumors, we found that ENDORSE scores were not significantly higher in tumors with
360 non-synonymous *PIK3CA* variants or activating *PIK3CA* variants that guide the use of
361 PI3K inhibitors (Supplementary Figure 3). Of the five significant genes, only tumors with
362 *TP53* mutations showed a significantly higher ENDORSE score (Figure 6b). We then
363 performed bootstrap analyses with the univariate Cox models of the significant genes
364 and found that none of the SNV Cox models performed better than the ENDORSE
365 model (Figure 6b).

366
367 Several gene-level amplifications were also associated with significant differences in
368 ENDORSE scores (Figure 6c, Supplementary Figure 4). Interestingly, the significant
369 amplifications were localized at chromosome 1q, 8p, 8q, or 11q, suggesting different
370 genetic alterations affecting a recurring set of loci may be correlated with the
371 emergence of resistance in the high-risk tumors (Figure 6c, Supplementary Table 12).
372 Like the univariate SNV models above, the univariate copy number alteration models
373 also performed poorly when compared to the ENDORSE model in bootstrap resampling
374 analyses (Figure 6d).

375



377 **Figure 6: Biology of the high-risk tumors.** A. Scatter plots displaying gene set
 378 enrichment scores (GES) of key pathways (X-axis) and ENDORSE scores (Y-axis). The
 379 cell cycle progression panel represents the hallmark G2M checkpoint signature, the

380 E2F1 upregulation panel represents E2F1_UP.V1_UP oncogenic (C6) signature and
381 the MTOR upregulation panel represents MTOR_UP.V1_UP oncogenic (C6) signature.
382 Blue lines with shading indicate generalized additive model fits with 95% C.I., with R^2
383 and p-values of the significant of the fit annotated on the panels. B. Barplots showing p-
384 values from the ANOVA analysis of ENDORSE scores with mutation status as the
385 grouping variable. The boxplot on the right shows difference in the ENDORSE scores
386 between *TP53* mutant and wildtype tumors. The lollipop plot below shows Somer's D_{xy}
387 of the univariate Cox models for the SNVs, with the vertical dotted line indicating D_{xy} of
388 the ENDORSE model. C. Ideograms showing mapped regions with copy number gains
389 that are significant in ANOVA analysis of ENDORSE scores with copy number gain
390 status as the grouping variables. Barplots on the right show p-values from the ANOVA
391 analysis. D. Lollipop plot showing Somer's D_{xy} of the univariate Cox models for the copy
392 number gains, with the vertical dotted line indicating D_{xy} of the ENDORSE model.
393

394 **DISCUSSION**

395 The criteria for classifying tumor as ER+ is based on a broad criteria of positive
396 immunohistochemical staining of 1-100% of cell nuclei for the estrogen receptor^{14,32}.
397 However, ER+ tumors are heterogeneous, both in terms of dependence on estrogen
398 signaling for growth and survival and intrinsic or acquired resistance to endocrine
399 therapy^{33,34}. Therefore, optimal clinical management of each ER+ breast cancer
400 depends on accurate prediction of response to endocrine therapy and selection of
401 companions for endocrine therapy. Several genomic tests are available for classifying
402 breast cancers into molecular subtypes³⁵ or assessing the likelihood of benefit from
403 chemotherapy in early-stage, node-negative ER+ breast cancers^{7,30}. Results from the
404 MINDACT and TAILORx studies^{7,8} show that it is possible for node-negative, early-
405 stage breast cancers to safely waive additional chemotherapy if they are predicted to be
406 at a low risk of recurrence based on genomic signatures. However, these tests have not
407 proven to be useful in the advanced and metastatic ER+ breast cancer setting. The
408 default primary treatment for advanced ER+ breast cancer remains endocrine therapy,
409 despite proven benefit from add-on targeted therapy or potential switch to
410 chemotherapy. Therefore, the key challenge in advanced ER+ breast cancer is to
411 stratify patients that will likely benefit from continued endocrine therapy and patients that
412 are likely resistant to single-agent endocrine therapy and will benefit from selecting a
413 different treatment strategy³⁶.

414

415 To address this challenge, we have developed a new prognostic model to predict
416 endocrine response in advanced ER+ breast cancers. We developed our model using

417 invasive tumors from the METABRIC study that were ER+ and included node-positive,
418 high-grade tumors. Our model addressed several challenges associated with the
419 development of genomic biomarkers. Since the number of available features to train the
420 genomic models tend to be much larger than the number of available samples ($p \gg n$),
421 it is quite easy to create complex prediction models that contain a large number of
422 predictor variables. Often, such models perform very well in the training datasets, but
423 the performance cannot be replicated in independent test datasets due to overfitting. A
424 number of approaches have been proposed to address this issue. Broadly, these can
425 be classified into unsupervised and supervised approaches. The unsupervised
426 approach typically relies on grouping or clustering the samples into based on similarity
427 of gene expression profiles, followed by analysis of association with survival outcomes
428 ³⁷. Alternatively, a supervised approach is to perform dimensionality reduction prior to
429 modelling the survival outcome or drug response using univariate or multivariate models
430 ³⁸. Our model utilized the later strategy by using a regularized Cox model for feature
431 selection, effectively reducing the dimensionality of the gene expression data. We
432 further collapsed the genes into a signature and parameterized the final Cox model on
433 the GES of the signatures. The rank-based approach to calculate GES also helped
434 mitigate issues associated with batch effects and differences in methods for
435 transcriptome profiling. We performed extensive performance evaluation of our model
436 against other published signatures and clinical factors. Consistently, we found that the
437 ENDORSE model was a better predictor than all other models in the training dataset
438 (Figure 2). Moreover, ENDORSE clearly outperformed all other published signatures
439 when they were applied to external validation datasets (Figures 3-5). Our results show

440 that ENDORSE is a highly accurate and reproducible model that outperforms current
441 approaches to predict endocrine response in metastatic ER+ breast cancer.

442
443 We also explored the biology of the ER+ tumors to identify possible mechanisms that
444 are commonly shared by high-risk tumor. We found that high-risk tumors showed a
445 consistent enrichment of pathways associated cell cycle progression and gain of
446 PI3K/MTOR signaling pathways (Figure 6a). In addition, we observed consistent gain of
447 the E2F1 signature, which may be associated with metastatic progression of breast
448 cancers^{39,40}. We also observed loss of Rb1 activity, which has been associated with
449 therapeutic resistance in ER+ breast cancers^{41,42}

450
451 In addition to common pathway phenotypes shared across high-risk tumors, mutations
452 in the *TP53* tumor suppressor genes were also significant (Figure 6b). Loss of function
453 *TP53* variants have long been associated with aggressiveness and chemotherapeutic
454 resistance in hormone-receptor negative breast cancers^{43,44}. However, recent studies
455 show that even though *TP53* mutations are infrequent in ER+ breast cancers, they have
456 similar negative impact on patient outcome as hormone-receptor negative breast
457 cancers⁴⁵. We also found recurrent copy number gains at chromosomes 8 and 11 to be
458 associated with high-risk tumors (Figure 6c). Amplifications at these loci have been
459 previously associated with aggressive and drug resistant cancers, and included several
460 oncogenes such as *MYC*, *CCND1* and multiple fibroblast growth factors^{46,47}. The
461 survival models based on genomic alterations were clearly outperformed by ENDORSE;

462 however, the recurrent nature of these alterations in high-risk tumors suggests further
463 studies to investigate their role in promoting endocrine resistance are warranted.
464
465 Drugs that target CDK4/6 to inhibit cell cycle activation⁴⁸, PI3K-inhibitors that target
466 tumor with activating *PIK3CA* mutations¹² and mTOR-inhibitors that prevent the
467 activation of mTOR signaling and cell proliferation¹³ have been studied and approved
468 for the treatment of advanced ER+ breast cancers in combination with endocrine
469 therapy. However, patients must first advance on primary endocrine therapy, with or
470 without additional CDK4/6 inhibitors, before they can be stratified in a different treatment
471 arm. Therefore, identifying high-risk tumors with the ENDORSE model prior to first-line
472 administration of single-agent endocrine therapy could help identify which cancers may
473 be better suited for an add-on regimen or switching to chemotherapy. Thus, future
474 clinical trials applying ENDORSE model may benefit from early and accurate prediction
475 of endocrine response in advanced, metastatic ER+ breast cancers. This could
476 ultimately help prolong survival of patients by stratifying in more appropriate treatment
477 group.
478

479 **METHODS**

480 **Data retrieval and pre-processing**

481 METABRIC gene expression, phenotypic and survival data were retrieved using
482 cBioPortal for cancer genomics⁴⁹. Independent validation datasets used in this study
483 were retrieved from the NCBI Gene Expression Omnibus database with the following
484 accession IDs: SET ER/PR GSE124647¹⁸, TransCONFIRM GSE76040¹⁹, and
485 ACOSOG Z1031B GSE87411³¹. For each gene expression dataset (log2 transformed),
486 we removed genes with zero variance and summarized genes with multiple probes by
487 mean expression and scaling of the expression levels of each gene to a mean of zero
488 and standard deviation of one.

489

490 **Inclusion criteria for METABRIC training cohort**

491 The METABRIC cohort contained a total of 2509 samples. Samples that met all of the
492 following criteria were included in the training cohort: patients that were ER-positive and
493 HER2-negative based on immunohistochemistry, patients that received hormone
494 therapy but did not receive additional chemotherapy, patients that were either alive or
495 died due to the disease and no other causes, and patients with complete survival and
496 transcriptomic data. After filtering, 833 samples were retained for model construction.

497

498 **Empirical signature and ENDORSE model construction**

499 The empirical gene signature was developed using a LASSO-regularized Cox
500 proportional hazards models, with OS as the outcome variable⁵⁰. The hazard function in
501 the Cox model is defined as:

$$h_i(t) = h_0(t)\exp(\beta x_i^T)$$

502 Where, X is a set of predictive gene expression features and h_0 is an arbitrary baseline
503 hazard function. The coefficient (β) for each predictor in the model can be estimated by
504 maximizing the partial likelihood function $L(\beta)$, defined as:

$$L(\beta) = \prod_i \frac{\exp(\beta x_{j(i)}^T)}{\sum_{l \in R_i} \exp(\beta x_l^T)}$$

505 Where R_i is the set of indices of observations failing (events) at time t_i . In the LASSO
506 Cox model, the regularized coefficient is obtained by adding a penalty parameter λ to
507 the log of the likelihood function.

$$\hat{\beta} = \min -\frac{1}{N}l(\beta) + \lambda \|\beta\|_1$$

508 Where, $l(\beta) = \log L(\beta)$. The λ penalty parameter was determined using 10-fold cross-
509 validation implemented in R package `glmnet`^{36,37}. The optimal λ minimized model
510 deviance.

511
512 We applied the model in a repeated (50 x 10-fold) cross validation framework. In each
513 iteration, a set of ‘seed genes’ or features with positive coefficients in the regularized
514 Cox model at a λ equal to one standard error from the minimum model deviance were
515 identified. The seed genes were expanded to a redundant correlation network by adding
516 all genes in the training transcriptome dataset that had Pearson’s correlation > 0.75 with
517 any of the seed genes. Across all iterations, we identified the common set of features
518 that were present in at least 50% of the correlation networks and defined this set of
519 features as the empirical signature.

520

521 The ENDORSE model was defined as the hazard's ratio of the Cox proportional
522 hazards model fitted on OS data of the training cohort with two components: GES for
523 the empirical gene signature and GES for the hallmark estrogen early response
524 signature.

$$h(t) = h_0(t) \times \exp(\beta_{emp}GES_{emp} + \beta_{er}GES_{er})$$

525 where, *emp* represents the empirical signature and *er* represents the estrogen response
526 signature.

527 For each signature, the GES were calculated for individual samples using the GSVA
528 package for R⁵³ using the ssGSEA method⁵⁴. The parameters for the ENDORSE model
529 were obtained by fitting the model to the full training cohort of 833 samples, resulting in
530 $\beta_{emp} = 1.54$ and $\beta_{er} = -2.72$.

531

532 **Models based on external signatures and clinical factors**

533 Clinical features such as tumor grade and mutation count, along with scores from
534 PAM50 and IntClust analyses were obtained directly from the METABRIC clinical
535 annotations accompanying the transcriptome data and were directly utilized in
536 univariate Cox models. Proliferation index based on the metaPCNA signature was
537 calculated using the R-package ProliferativeIndex²⁷.

538 We replicated the signatures and algorithms developed in the TransCONFIRM, SET
539 ER/PR and 21-gene prognostic signature studies by following the methods described in
540 the respective studies. The TransCONFIRM signature composed of 37 genes was
541 implemented by performing hierarchical clustering of the gene expression data using
542 these genes and cutting the tree ($k=2$) to stratify samples in high or low TransCONFIRM

543 score categories. The SET signature was implemented by calculating (the average
544 expression of the 18-genes in the signature) – (the expression of 10 house-keeping
545 genes) + 2. The 21-gene signature (ODX) score was calculated by following the
546 unscaled risk score calculation reported by the study. *BAG1* transcript was missing from
547 the METABRIC cohort and was not included in the unscaled score calculation. Since
548 this transcript was uniformly missing on all samples, the relative risk scores could be
549 compared across the samples.

550

551 **Cox model performance evaluation in training data**

552 The predictive ability of ENDORSE and various other models were evaluated in the
553 METABRIC training dataset using a bootstrap resampling analysis of the Cox
554 regression models. The resampling was repeated 150 times for each model and a
555 Somer's D_{xy} rank correlation was calculated in each repeat. A final bias-corrected index
556 of Somer's D_{xy} was obtained as measure of the model's predictive ability. The bootstrap
557 resampling and calculations of the Somer's D_{xy} were performed using the R package
558 'rms'. Models based on SNVs and CNAs significantly associated with ENDORSE scores
559 were also evaluated by obtaining Somer's D_{xy} rank correlation metric of the univariate
560 Cox model.

561

562 To compare each of the external signatures and clinical feature models with the
563 ENDORSE model, we applied Vuong's⁵⁵ partial likelihood ratio test for non-nested Cox
564 regression models calculated using the R package 'nonnestcox'
565 (<https://github.com/thomashielscher/nonnestcox/>). The individual components of the

566 ENDORSE model were compared to the full model using likelihood ratio tests for nested
567 Cox models.

568

569 **Model validation in independent datasets**

570 We compared the predictive performance of ENDORSE in multiple independent
571 datasets. First, we integrated the training (METABRIC) and test (independent validation)
572 datasets to perform batch correction using the ComBat function of the R package 'sva
573 ⁵⁶. Next, we calculated the GES for the ENDORSE signatures in the training
574 (METABRIC) and test (independent validation) splits of the batch-corrected gene
575 expression dataset. Then, the parameters of the ENDORSE Cox model were calculated
576 on the batch-corrected training split with the OS information as the response variable.
577 Finally, the parameterized Cox model was applied to the test split to obtain a predicted
578 risk score.

579

580 In case of the SET ER/PR cohort, we used the predicted ENDORSE risk scores to
581 stratify the patients into risk categories, with an ENDORSE score ≥ 2 representing the
582 high-risk group, ≤ 1 representing the low-risk group and other intermediate values
583 representing the medium risk group. We compared the significance of stratification of
584 both OS and PFS curves based on ENDORSE, SET and TransCONFIRM scores using
585 log-rank tests. Further, we compared the models using partial likelihood ratio tests for
586 non-nested Cox models.

587

588 For the TransCONFIRM and ACOSOG cohorts, we compared the ENDORSE risk
589 scores, SET and TransCONFIRM predictions with reported clinical variables, such as
590 percentage of cells positive for Ki67 at the end of treatment and clinical outcomes using
591 generalized linear models for continuous outcome variables or one-way ANOVA
592 analysis for categorical outcomes.

593

594 **Biological features associated with ENDORSE scores**

595 To determine the possible biological mechanisms associated with emergence of
596 endocrine resistance and high ENDORSE risk scores, we evaluated the enrichment
597 scores of various biological pathway and oncogenic signatures across the training and
598 independent validation cohorts. We used the ssGSEA method to obtain GES for
599 hallmark, curated (C2) and oncogenic signature (C6) gene sets from the molecular
600 signatures database⁵⁷. For each signature, we fitted a generalized additive model
601 against the predicted ENDORSE score to obtain significance of the fit, R^2 and
602 proportion of variance explained by the model. None of the curated signatures were
603 significant in the METABRIC analyses and were excluded from further consideration in
604 the independent validation datasets.

605

606 Gene-level somatic SNV and CNV analyses were performed using data reported by the
607 METABRIC study. SNV's were retained based on a mutation frequency of ≥ 5 across all
608 samples and limited to genes that are known cancer-related genes. Pathogenic *PIK3CA*
609 variants associated with PI3K inhibitor sensitivity were obtained from the drug labels for
610 alpelisib based on the SOLAR1 clinical trial¹². Significant SNVs and CNVs were

611 obtained using a one-way ANOVA analysis of the ENDORSE scores with mutation
612 status as the factor.

613

614 **Data availability and code**

615 All training and validation datasets used in this study are publicly available and listed
616 under “data retrieval, preprocessing and analysis”. All analyses were performed in
617 RStudio (1.2.5033, R 3.6.3). The sample code for reproducing the analyses in this study
618 are available at https://osf.io/bd3m7/?view_only=da4f860bd2474745880944fce1d433b1

619

620 **ACKNOWLEDGEMENTS**

621 Funding for this research was provided by the National Cancer Institute of the National
622 Institutes of Health through the U54 grant 1U54CA209978.

623

624 **AUTHOR CONTRIBUTIONS**

625 Conceptualization, Methodology, Investigation – AN, ALC, AHB; Data Curation, Formal
626 Analysis, Software, Visualization, Validation – AN; Funding Acquisition, Resources,
627 Supervision, Project Administration – ALC, AHB; Writing – original draft – AN; Writing –
628 review & editing – AN, ALC, AHB.

629

630 **CONFLICT OF INTERESTS**

631 The authors declare that they have no conflict of interest.

632 **REFERENCES**

- 633 1. Sung, H. *et al.* Global Cancer Statistics 2020: GLOBOCAN Estimates of Incidence
634 and Mortality Worldwide for 36 Cancers in 185 Countries. *CA A Cancer J Clin* **71**,
635 209–249 (2021).
- 636 2. Harvey, J. M., Clark, G. M., Osborne, C. K. & Allred, D. C. Estrogen receptor status
637 by immunohistochemistry is superior to the ligand-binding assay for predicting
638 response to adjuvant endocrine therapy in breast cancer. *J. Clin. Oncol.* **17**, 1474–
639 1481 (1999).
- 640 3. Kohler, B. A. *et al.* Annual Report to the Nation on the Status of Cancer, 1975-2011,
641 Featuring Incidence of Breast Cancer Subtypes by Race/Ethnicity, Poverty, and
642 State. *JNCI: Journal of the National Cancer Institute* **107**, (2015).
- 643 4. Waks, A. G. & Winer, E. P. Breast Cancer Treatment: A Review. *JAMA* **321**, 288
644 (2019).
- 645 5. McDonnell, D. P. & Wardell, S. E. The molecular mechanisms underlying the
646 pharmacological actions of ER modulators: implications for new drug discovery in
647 breast cancer. *Current Opinion in Pharmacology* **10**, 620–628 (2010).
- 648 6. Smith, I. E. & Dowsett, M. Aromatase Inhibitors in Breast Cancer. *N Engl J Med* **348**,
649 2431–2442 (2003).
- 650 7. Cardoso, F. *et al.* 70-Gene Signature as an Aid to Treatment Decisions in Early-
651 Stage Breast Cancer. <https://doi.org/10.1056/NEJMoa1602253>
652 <https://www.nejm.org/doi/10.1056/NEJMoa1602253> (2016)
653 doi:10.1056/NEJMoa1602253.

- 654 8. Sparano, J. A. *et al.* Adjuvant Chemotherapy Guided by a 21-Gene Expression Assay
655 in Breast Cancer. *New England Journal of Medicine* **379**, 111–121 (2018).
- 656 9. Krop, I. *et al.* Use of Biomarkers to Guide Decisions on Adjuvant Systemic Therapy
657 for Women With Early-Stage Invasive Breast Cancer: American Society of Clinical
658 Oncology Clinical Practice Guideline Focused Update. *JCO* **35**, 2838–2847 (2017).
- 659 10. Duffy, M. J. *et al.* Clinical use of biomarkers in breast cancer: Updated guidelines
660 from the European Group on Tumor Markers (EGTM). *European Journal of Cancer*
661 **75**, 284–298 (2017).
- 662 11. McAndrew, N. P. & Finn, R. S. Management of ER positive metastatic breast
663 cancer. *Seminars in Oncology* **47**, 270–277 (2020).
- 664 12. André, F. *et al.* Alpelisib for PIK3CA-Mutated, Hormone Receptor–Positive
665 Advanced Breast Cancer. *New England Journal of Medicine* **380**, 1929–1940 (2019).
- 666 13. Baselga, J. *et al.* Everolimus in Postmenopausal Hormone-Receptor–Positive
667 Advanced Breast Cancer. *N Engl J Med* **366**, 520–529 (2012).
- 668 14. Rugo, H. S. *et al.* Endocrine Therapy for Hormone Receptor–Positive Metastatic
669 Breast Cancer: American Society of Clinical Oncology Guideline. *JCO* **34**, 3069–3103
670 (2016).
- 671 15. Gradishar, W. J. *et al.* NCCN Guidelines Insights: Breast Cancer, Version
672 1.2017. *J Natl Compr Canc Netw* **15**, 433–451 (2017).
- 673 16. Gradishar, W. J. *et al.* Breast Cancer, Version 3.2020, NCCN Clinical Practice
674 Guidelines in Oncology. *Journal of the National Comprehensive Cancer Network* **18**,
675 452–478 (2020).

- 676 17. Cardoso, F. *et al.* 5th ESO-ESMO international consensus guidelines for
677 advanced breast cancer (ABC 5). *Annals of Oncology* **31**, 1623–1649 (2020).
- 678 18. Sinn, B. V. *et al.* SET ER/PR: a robust 18-gene predictor for sensitivity to
679 endocrine therapy for metastatic breast cancer. *NPJ Breast Cancer* **5**, 16 (2019).
- 680 19. Jeselsohn, R. *et al.* TransCONFIRM: Identification of a Genetic Signature of
681 Response to Fulvestrant in Advanced Hormone Receptor-Positive Breast Cancer.
682 *Clin. Cancer Res.* **22**, 5755–5764 (2016).
- 683 20. Boutros, P. C. The path to routine use of genomic biomarkers in the cancer clinic.
684 *Genome Res* **25**, 1508–1513 (2015).
- 685 21. Witten, D. M. & Tibshirani, R. Survival analysis with high-dimensional covariates.
686 *Stat Methods Med Res* **19**, 29–51 (2010).
- 687 22. Taylor, J. M. G., Ankerst, D. P. & Andridge, R. R. Validation of Biomarker-Based
688 Risk Prediction Models. *Clin Cancer Res* **14**, 5977–5983 (2008).
- 689 23. Pereira, B. *et al.* The somatic mutation profiles of 2,433 breast cancers refine
690 their genomic and transcriptomic landscapes. *Nature Communications* **7**, 1–16
691 (2016).
- 692 24. Curtis, C. *et al.* The genomic and transcriptomic architecture of 2,000 breast
693 tumours reveals novel subgroups. *Nature* **486**, 346–352 (2012).
- 694 25. Liberzon, A. *et al.* The Molecular Signatures Database Hallmark Gene Set
695 Collection. *Cell Systems* **1**, 417–425 (2015).
- 696 26. Venet, D., Dumont, J. E. & Detours, V. Most Random Gene Expression
697 Signatures Are Significantly Associated with Breast Cancer Outcome. *PLOS*
698 *Computational Biology* **7**, e1002240 (2011).

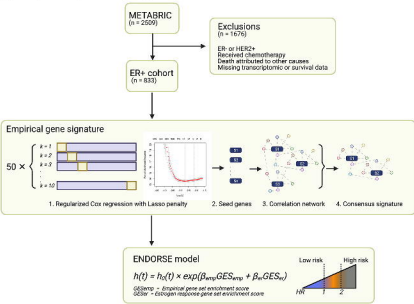
- 699 27. Ramaker, R. C. *et al.* RNA sequencing-based cell proliferation analysis across 19
700 cancers identifies a subset of proliferation-informative cancers with a common
701 survival signature. *Oncotarget* **8**, 38668–38681 (2017).
- 702 28. Nielsen, T. O. *et al.* A Comparison of PAM50 Intrinsic Subtyping with
703 Immunohistochemistry and Clinical Prognostic Factors in Tamoxifen-Treated
704 Estrogen Receptor–Positive Breast Cancer. *Clin Cancer Res* **16**, 5222–5232 (2010).
- 705 29. Dawson, S.-J., Rueda, O. M., Aparicio, S. & Caldas, C. A new genome-driven
706 integrated classification of breast cancer and its implications. *EMBO J* **32**, 617–628
707 (2013).
- 708 30. Paik, S. *et al.* A multigene assay to predict recurrence of tamoxifen-treated,
709 node-negative breast cancer. *N. Engl. J. Med.* **351**, 2817–2826 (2004).
- 710 31. Ellis, M. J. *et al.* Ki67 Proliferation Index as a Tool for Chemotherapy Decisions
711 During and After Neoadjuvant Aromatase Inhibitor Treatment of Breast Cancer:
712 Results From the American College of Surgeons Oncology Group Z1031 Trial
713 (Alliance). *J. Clin. Oncol.* **35**, 1061–1069 (2017).
- 714 32. Allison, K. H. *et al.* Estrogen and Progesterone Receptor Testing in Breast
715 Cancer: ASCO/CAP Guideline Update. *JCO* **38**, 1346–1366 (2020).
- 716 33. Musgrove, E. A. & Sutherland, R. L. Biological determinants of endocrine
717 resistance in breast cancer. *Nature Reviews Cancer* **9**, 631–643 (2009).
- 718 34. Spoerke, J. M. *et al.* Heterogeneity and clinical significance of ESR1 mutations in
719 ER-positive metastatic breast cancer patients receiving fulvestrant. *Nature*
720 *Communications* **7**, 1–10 (2016).

- 721 35. Parker, J. S. *et al.* Supervised Risk Predictor of Breast Cancer Based on Intrinsic
722 Subtypes. *J Clin Oncol* **27**, 1160–1167 (2009).
- 723 36. Hart, C. D. *et al.* Challenges in the management of advanced, ER-positive,
724 HER2-negative breast cancer. *Nat Rev Clin Oncol* **12**, 541–552 (2015).
- 725 37. Sotiriou, C. *et al.* Breast cancer classification and prognosis based on gene
726 expression profiles from a population-based study. *PNAS* **100**, 10393–10398 (2003).
- 727 38. Paul, D., Bair, E., Hastie, T. & Tibshirani, R. “Preconditioning” for feature
728 selection and regression in high-dimensional problems. *Ann. Statist.* **36**, 1595–1618
729 (2008).
- 730 39. Hollern, D. P., Honeysett, J., Cardiff, R. D. & Andrechek, E. R. The E2F
731 Transcription Factors Regulate Tumor Development and Metastasis in a Mouse
732 Model of Metastatic Breast Cancer. *Molecular and Cellular Biology* **34**, 3229–3243
733 (2014).
- 734 40. Hollern, D. P. *et al.* E2F1 Drives Breast Cancer Metastasis by Regulating the
735 Target Gene FGF13 and Altering Cell Migration. *Sci Rep* **9**, 10718 (2019).
- 736 41. Bosco, E. E. *et al.* The retinoblastoma tumor suppressor modifies the therapeutic
737 response of breast cancer. *J Clin Invest* **117**, 218–228 (2007).
- 738 42. Witkiewicz, A. K. & Knudsen, E. S. Retinoblastoma tumor suppressor pathway in
739 breast cancer: prognosis, precision medicine, and therapeutic interventions. *Breast*
740 *Cancer Research* **16**, 207 (2014).
- 741 43. Cattoretti, G., Rilke, F., Andreola, S., D’Amato, L. & Delia, D. P53 expression in
742 breast cancer. *International Journal of Cancer* **41**, 178–183 (1988).

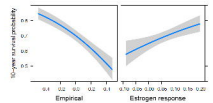
- 743 44. Elledge, R. M. *et al.* Prognostic significance of p53 gene alterations in node-
744 negative breast cancer. *Breast Cancer Res Tr* **26**, 225–235 (1993).
- 745 45. Ungerleider, N. A. *et al.* Breast cancer survival predicted by TP53 mutation status
746 differs markedly depending on treatment. *Breast Cancer Research* **20**, 115 (2018).
- 747 46. Baslan, T. *et al.* Novel insights into breast cancer copy number genetic
748 heterogeneity revealed by single-cell genome sequencing. *eLife* **9**, e51480 (2020).
- 749 47. Lundgren, K., Holm, K., Nordenskjöld, B., Borg, Å. & Landberg, G. Gene
750 products of chromosome 11q and their association with CCND1 gene amplification
751 and tamoxifen resistance in premenopausal breast cancer. *Breast Cancer Res* **10**,
752 R81 (2008).
- 753 48. Hortobagyi, G. N. *et al.* Ribociclib as First-Line Therapy for HR-Positive,
754 Advanced Breast Cancer. *N Engl J Med* **375**, 1738–1748 (2016).
- 755 49. Gao, J. *et al.* Integrative analysis of complex cancer genomics and clinical
756 profiles using the cBioPortal. *Sci Signal* **6**, p11 (2013).
- 757 50. Tibshirani, R. Regression Shrinkage and Selection Via the Lasso. *Journal of the*
758 *Royal Statistical Society: Series B (Methodological)* **58**, 267–288 (1996).
- 759 51. Friedman, J. H., Hastie, T. & Tibshirani, R. Regularization Paths for Generalized
760 Linear Models via Coordinate Descent. *Journal of Statistical Software* **33**, 1–22
761 (2010).
- 762 52. Simon, N., Friedman, J. H., Hastie, T. & Tibshirani, R. Regularization Paths for
763 Cox's Proportional Hazards Model via Coordinate Descent. *Journal of Statistical*
764 *Software* **39**, 1–13 (2011).

- 765 53. Hänzelmann, S., Castelo, R. & Guinney, J. GSVA: gene set variation analysis for
766 microarray and RNA-Seq data. *BMC Bioinformatics* **14**, 7 (2013).
- 767 54. Barbie, D. A. *et al.* Systematic RNA interference reveals that oncogenic KRAS -
768 driven cancers require TBK1. *Nature* **462**, 108–112 (2009).
- 769 55. Vuong, Q. H. Likelihood Ratio Tests for Model Selection and Non-Nested
770 Hypotheses. *Econometrica* **57**, 307 (1989).
- 771 56. Leek, J. T., Johnson, W. E., Parker, H. S., Jaffe, A. E. & Storey, J. D. The sva
772 package for removing batch effects and other unwanted variation in high-throughput
773 experiments. *Bioinformatics* **28**, 882–883 (2012).
- 774 57. Liberzon, A. *et al.* Molecular signatures database (MSigDB) 3.0. *Bioinformatics*
775 **27**, 1739–1740 (2011).
- 776

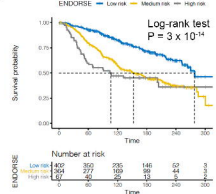
A Empirical signature development and ENDORSE model



B Predicted survival probabilities

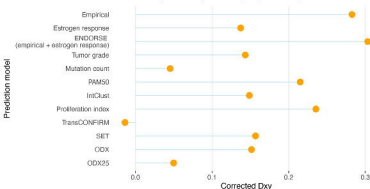


C METABRIC cohort (ER+/HER2-, n = 833)



METABRIC cohort (ER+/HER2-, n = 833)

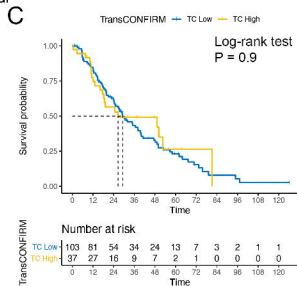
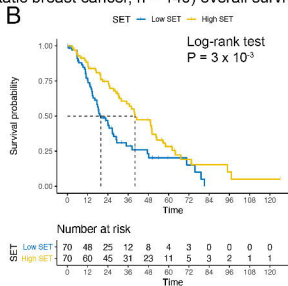
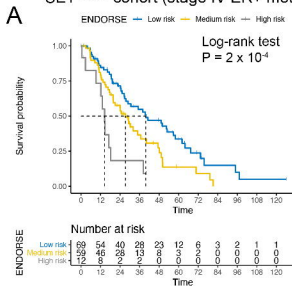
A Prediction model validation (bootstrap resampling, B=150)



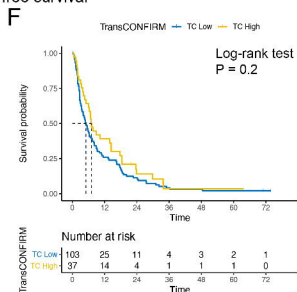
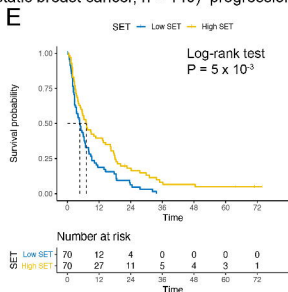
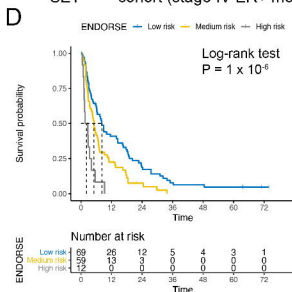
B Model comparisons

Model 1	Model 2	Variance test <i>H1: Model 1 and Model 2 are distinguishable</i>	Likelihood ratio test (nested) <i>H1A: Full model fits better than reduced model</i>	Partial likelihood ratio test (non-nested) <i>H1A: Model 1 fits better than Model 2</i>
ENDORSE	Empirical	1.47×10^{-3}	1.09×10^{-3}	
	Estrogen response	3.83×10^{-6}	3.93×10^{-14}	
METABRIC tumor characteristics and signatures				
	Tumor grade	$< 2 \times 10^{-16}$		2.08×10^{-3}
	Mutation count	$< 2 \times 10^{-16}$		9.76×10^{-6}
	PAM50	2.22×10^{-8}		0.033
	IntClust	$< 2 \times 10^{-16}$		0.02
	Proliferation index	3.73×10^{-6}		4.42×10^{-6}
External signatures				
	TransCONFIRM	1.67×10^{-7}		9.73×10^{-6}
	SET	$< 2 \times 10^{-16}$		3.53×10^{-6}
	ODX	2.18×10^{-7}		6.15×10^{-6}
	ODX25	1.49×10^{-6}		1.32×10^{-6}

SET^{ER/PR} cohort (stage IV ER+ metastatic breast cancer, n = 140) overall survival



SET^{ER/PR} cohort (stage IV ER+ metastatic breast cancer, n = 140) progression-free survival

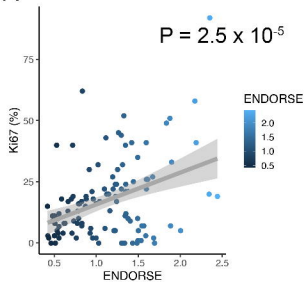


G

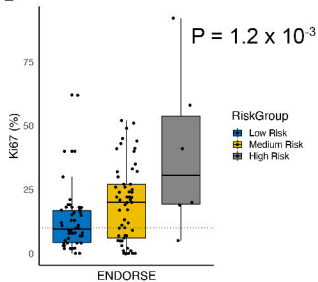
	Model 1	Model 2	Variance test <i>H1: Model 1 and Model 2 are distinguishable</i>	Partial likelihood ratio test (non-nested) <i>H1A: Model 1 fits better than Model 2</i>
ENDORSE	Overall survival			
	SET		2.1×10^{-4}	0.667
	TransCONFIRM		2.6×10^{-3}	0.046
ENDORSE	Progression free survival			
	SET		1.2×10^{-5}	0.258
	TransCONFIRM		9×10^{-6}	0.038

TransCONFIRM cohort (ER+ metastatic breast cancer, n = 112)

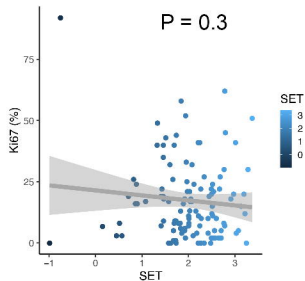
A



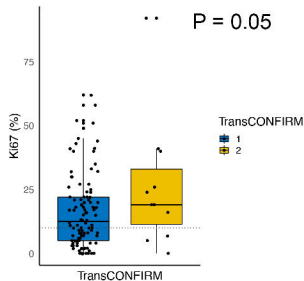
B



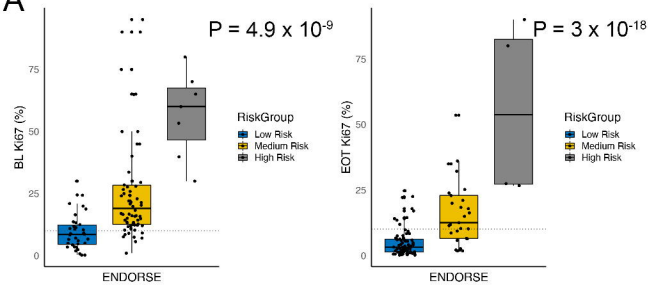
C



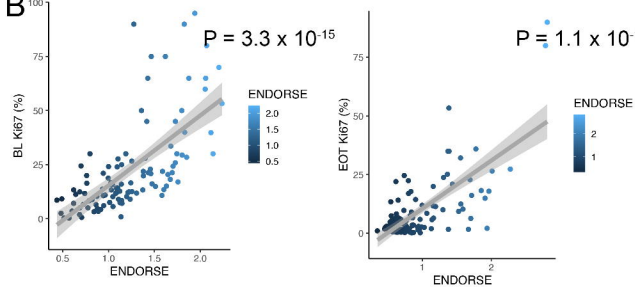
D



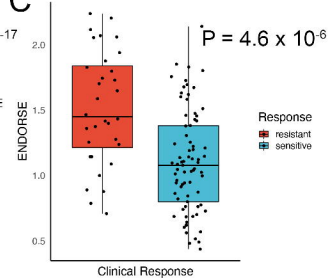
A



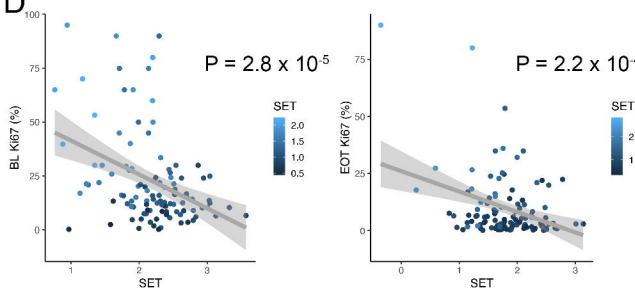
B



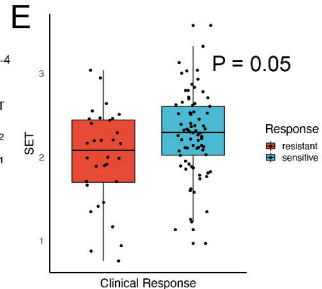
C



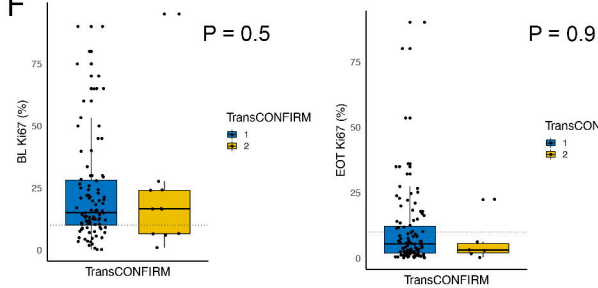
D



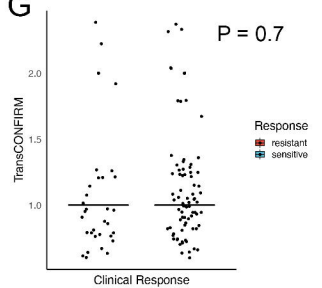
E

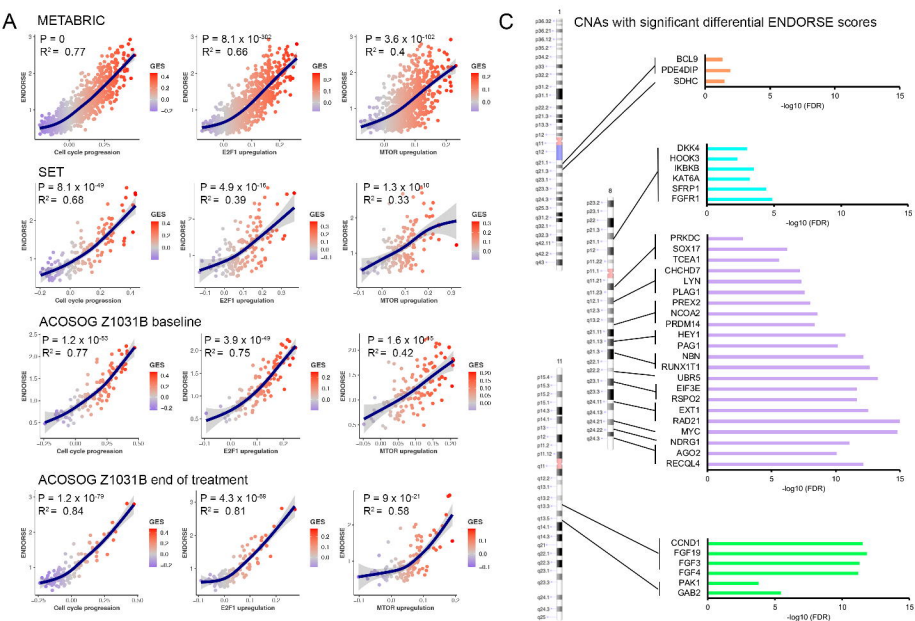


F

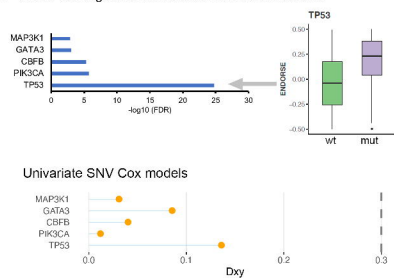


G





B SNVs with significant differential ENDORSE scores



D Univariate CNA Cox models

